

ARMY RESEARCH LABORATORY



Yaw Card Influence on Stability and Yaw Growth for Spin- Stabilized Projectiles

Gene R. Cooper
Kevin S. Fansler

ARL-TR-1431

AUGUST 1997

19970909 099

DTIC QUALITY INSPECTED 3

Approved for public release; distribution is unlimited.

The findings in this report are not to be construed as an official Department of the Army position unless so designated by other authorized documents.

Citation of manufacturer's or trade names does not constitute an official endorsement or approval of the use thereof.

Destroy this report when it is no longer needed. Do not return it to the originator.

Army Research Laboratory

Aberdeen Proving Ground, MD 21005-5066

ARL-TR-1431

August 1997

Yaw Card Influence on Stability and Yaw Growth for Spin-Stabilized Projectiles

Gene R. Cooper
Kevin S. Fansler
Weapons & Materials Research Directorate

Approved for public release; distribution is unlimited.

DTIC QUALITY INSPECTED 3

Abstract

Using an impulse or Dirac delta approach, the stability and growth of yaw for a spin-stabilized projectile as it transits a yaw card range is investigated. The card-induced changes in the complex yaw arm amplitudes and phases are expressed as difference equations. For a yaw card range with uniform spacings, the solutions to the general difference equations yield the magnitude and phase values for the complex yawing arms as a function of the card index number. A stepwise encounter with a yaw card reduces the epicyclical phase values across the yaw card. The parameters for the solution include encounter phase value at the entrance of the range, the characteristics of the yaw card, and the distance between the cards. Critical curves separating stable and unstable flight are presented as a function of yaw card spacing and a stability parameter that depends upon both the flight characteristics of the projectile and the card material and thickness. Quasi-universal curves of a transformed epicyclical phase encounter value versus a normalized epicyclical phase reduction value are graphically presented.

ACKNOWLEDGMENTS

We wish to thank Dr. Aivars Celmins and Dr. James Danberg for their comments and suggestions to improve this work.

INTENTIONALLY LEFT BLANK

TABLE OF CONTENTS

	<u>Page</u>
LIST OF FIGURES	vii
1. INTRODUCTION	1
2. THE DIFFERENTIAL EQUATION OF MOTION FOR PROJECTILES FIRED THROUGH YAW CARDS	2
3. DIFFERENCE EQUATIONS FOR THE DIRAC DELTA APPROACH	3
3.1 Modal Parameters Before and After Interaction	5
3.2 Solution for Uniform Yaw Card Range With Difference Equations	7
4. STABILITY BOUNDARIES AND GROWTH IN YAW	10
5. FURTHER DISCUSSION AND ILLUSTRATIONS	18
6. SUMMARY AND CONCLUSIONS	21
7. REFERENCES	23
LIST OF SYMBOLS	25
DISTRIBUTION LIST	29
REPORT DOCUMENTATION PAGE	35

INTENTIONALLY LEFT BLANK.

LIST OF FIGURES

<u>Figure</u>		<u>Page</u>
1	Normalized Phase Jump And Modal Arm Amplitude Versus the Epicyclic Phase Encounter Value ($\mu = 0.1$).	6
2	Stable and Unstable Regions as a Function of μ	11
3	Comparison Between Approximate and Exact Solution for the Stability Boundary.	12
4	Stationary Phase Encounter Values Versus the Phase Interval with the Superimposed Curve for the Fractional Change in the Modal Arm Amplitudes ($\mu = 0.1$).	14
5	Normalized Phase Jump and Modal Amplitude Change Versus the Quasi-Universal Transformed Card Encounter Phase Values.	16
6	Phase Encounter Value Versus Card Index Number.	17
7	Comparisons of Stable Epicyclic Motion for the 7.62-mm Projectile.	18
8	Maximum Growth of Fast Modal Arm.	19
9	Maximum Decay of Fast Modal Arm Amplitude.	20
10	Unstable Epicyclic Motion for a 7.62-mm Projectile.	21

INTENTIONALLY LEFT BLANK.

YAW CARD INFLUENCE ON STABILITY AND YAW GROWTH FOR SPIN-STABILIZED PROJECTILES

1. INTRODUCTION

Yaw card arrays set up at equal intervals on a firing range have been used to obtain flight data when spark ranges are not available or when the spark range operations could be compromised. The interactions of the projectile with the yaw cards cause the reduced flight coefficients to differ from the spark range values. McCoy (1992) used a Fourier analysis approach and assumed that the fluctuating details generated by the yaw card interactions would average zero, thereby obtaining an average phase shift for each projectile-card interaction. These projectile flight data, when reduced and corrected for the yaw card interactions, predicted the flight coefficient values obtained in a spark photography range. Cooper and Fansler (1997), using a Dirac delta approach, considered the individual interactions of the projectile with each yaw card and calculated the fast and slow arm magnitudes at each card along with the phase changes. With the new approach, they were able to examine the variations from the average value at each card. The calculations for a given card depended upon the calculation obtained for the previous card. In turn, the previous card calculation depended upon the adjacent card before it. Thus, calculations needed to be performed for all the cards, beginning at the first card. For small perturbations, they obtained the correction needed to reduce the yaw card range flight data to the equivalent spark range data, which was previously obtained using McCoy's (1992) approach. Thus, the correction is only valid for small perturbations, or equivalently, sufficiently thin yaw cards.

Because the material comprising the yaw cards is dense, it is reasonable to expect that decreasing the spacing of the yaw cards sufficiently or using thick yaw cards might result in destabilizing the flight of projectiles through the range. In particular, marginally stable projectiles would require careful design of the range to avoid inducing instability. McCoy (1992) asserted that the usual stability criterion, extended with his correction to the moment for the yaw card range, was still valid. Cooper and Fansler (1997) validated the assertion by calculating the unstable growth that met McCoy's criterion for instability. They also pointed out that the obtained expression was actually an approximation valid only for small values of the stability parameter, which is equivalent to assuming that the yaw cards are sufficiently thin. Cooper and Fansler also calculated the card-by-card growth of a projectile's yaw in a range that has its card spacing corresponding to nearly the optimum condition for maximum amplitude increase for the modal arm amplitudes. They could also examine the detailed yawing for a projectile that entered the range at different initial epicyclic phase

values, both for stable and unstable flight.

The current approach is a continuation of the work by Cooper and Fansler (1997). As before, interactions with the yaw cards are treated as discrete impulses, but now a yaw card range with equal intervals between yaw cards is assumed. This approach yields second order difference equations with known solutions. With solutions for the second order difference equations known, it is no longer necessary to know the behavior of the projectile at all the preceding yaw cards. In this report, the boundaries between stable and unstable flight are determined along with the growth rate for yaw modal arm amplitude and its dependence on various parameters. These expressions are valid for both small and large values of the stability parameter. Quasi-universal functions are obtained, giving the relationships between the phase encounter value at each card, the epicyclic phase jump value, and the change in the modal arm magnitudes caused by the card encounter.

2. THE DIFFERENTIAL EQUATION OF MOTION FOR PROJECTILES FIRED THROUGH YAW CARDS

The differential equation of pitching and yawing motion for a spinning, symmetric projectile, acted upon by a linear pitching moment and neglecting damping processes is given in Murphy's notation (1963):

$$\tilde{\xi}'' - iP\tilde{\xi}' - M\tilde{\xi} = 0, \quad (1)$$

in which

$$\begin{aligned} \tilde{\xi} &= \sin \beta + i \sin \alpha, \text{ the complex yaw,} \\ P &= \frac{I_x p d}{I_y V} \\ M &= \frac{\rho A d^3}{2I_y} C_{M\alpha}, \\ I_x &= \text{axial moment of inertia,} \\ I_y &= \text{transverse moment of inertia,} \\ d &= \text{projectile reference diameter,} \\ p &= \text{axial spin} \\ \rho &= \text{air density,} \\ A &= \pi d^2/4, \text{ reference area,} \\ C_{M\alpha} &= \text{aerodynamic pitching moment coefficient,} \end{aligned}$$

and the independent variable is the distance in calibers. For this report, it is assumed that the amplitude of the complex yaw is small enough that $\sin \alpha \approx \alpha$ and $\sin \beta \approx \beta$. Only the first order aerodynamic coefficients are then used.

Equation (1) is the equation of motion in air but the yaw card range has cards consisting of dense material at various spacings. Following Cooper and Fansler (1997), a nondimensional card-overturning moment can be defined for the card material, similarly to M :

$$M_c \equiv \frac{\rho_c A d^3}{2I_y} C_{M\alpha_c}. \quad (2)$$

The corresponding nondimensional impulse for the card-overturning moment is defined as

$$\mathcal{I}_c \equiv \frac{\rho_c A d^2 \tau_c}{2I_y} C_{M\alpha_c}, \quad (3)$$

and the independent variable is the distance, s , in calibers.

For the yaw card range, Equation (1) must be modified to account for the yaw card interactions. As discussed in the preceding section, each yaw card transmits an overturning moment to the projectile, which can be modeled as an impulse located at the position s_j , which is the arclength traveled by the projectile, given in calibers. The Dirac delta function (Dennery & Kryzwicki 1967) is used with the pitching moment impulse value, and the interactions of these yaw cards with a projectile are represented by replacing M with $M + \mathcal{I}_c \sum_{j=1}^n \delta(s - s_j)$. Equation (1) is replaced with

$$\tilde{\xi}'' - iP\tilde{\xi}' - [M + \mathcal{I}_c \sum_{j=1}^n \delta(s - s_j)]\tilde{\xi} = 0. \quad (4)$$

3. DIFFERENCE EQUATIONS FOR THE DIRAC DELTA APPROACH

The solution of Equation (4) in the interval between the j th card and the j th + 1 card is, as given by an extension of Murphy's notation (1963):

$$\tilde{\xi} = K_{1,j} e^{i\phi_{1,j}} e^{i\phi'_1 s} + K_{2,j} e^{i\phi_{2,j}} e^{i\phi'_2 s}, \quad j = 0, 1, \dots, n-1, \quad (5)$$

in which $\phi_{1,j}$ and $\phi_{2,j}$ are the card-modified initial phase angles of the fast modal arm and the slow modal arm, respectively, after interaction with the j th yaw card but before interaction with the j th + 1 yaw card. The phase angular velocities for the fast and slow modal arms, ϕ'_1 and ϕ'_2 , are

$$\phi'_1 = \frac{1}{2}P + \frac{1}{2}\sqrt{P^2 - 4M}, \quad (6)$$

$$\phi'_2 = \frac{1}{2}P - \frac{1}{2}\sqrt{P^2 - 4M}. \quad (7)$$

It is assumed that the projectile is spin stabilized and is gyroscopically stable while traveling through the air. This stable condition requires that $\sqrt{P^2 - 4M}$ is real and, in turn, implies that the values of ϕ'_1 and ϕ'_2 are real. To achieve stable flight, even in cold and dense air, the axial angular velocity, p , must be large enough so that a comfortable margin of stability is achieved. Good margins of stability are achieved for most projectiles with twist designs varying from one revolution in seven bore diameters to one revolution in 20 calibers. Likewise, $K_{1,j}$ and $K_{2,j}$ are the fast modal arm and slow modal arm amplitudes, respectively, after interaction with the j th yaw card but before interaction with the j th + 1 yaw card. The value of j can be zero, which indicates that the projectile has not yet interacted with a yaw card. Equation (5) describes the motion of an epicycloid in which both modal arms are moving. Equation (5) can be rearranged to illustrate the salient aspects of the motion as it relates to yaw cards:

$$\tilde{\xi} = K_{2,j} e^{i\phi_{2,j}} e^{i\phi'_2 s} \left[\frac{K_{1,j}}{K_{2,j}} e^{i(\phi_{1,j} - \phi_{2,j})} e^{i(\phi'_1 - \phi'_2)s} + 1 \right], \quad (8)$$

in which we use the relationship, $\phi'_1 - \phi'_2 = \sqrt{P^2 - 4M}$. Equation(8) shows that if the observer moves with the slow arm, a circle is completed in the distance interval, $\Delta s = (2\pi)/(\sqrt{P^2 - 4M})$. The superimposed circle constitutes an epicycle. For a statically unstable projectile, both arms move in the same direction. The phase angle value of the first term in brackets when the projectile encounters a yaw card will determine the impulsive forces on the projectile. Consider when $K_{1,j} = K_{2,j}$. When the epicyclic phase angle, $\phi_{1,j} - \phi_{2,j} + (\phi'_1 - \phi'_2)s$, equals zero, the modal arms are aligned in the same direction and $d|\tilde{\xi}|/ds = 0$. When the phase angle equals $\pi/2$, $d|\tilde{\xi}|/ds$ is decreasing most rapidly. When the phase angle equals π , the total yaw and $d|\tilde{\xi}|/ds$ are zero. When the epicyclic phase angle equals $3\pi/2$, $d|\tilde{\xi}|/ds$ is increasing most rapidly.

For convenience, the complex modal arms are defined as

$$\mathcal{K}_{1,j} \equiv K_{1,j} e^{i\phi_{1,j}}, \quad (9)$$

$$\mathcal{K}_{2,j} \equiv K_{2,j} e^{i\phi_{2,j}}. \quad (10)$$

With the above definitions, Equation (5) becomes

$$\tilde{\xi} = \mathcal{K}_{1,j} e^{i\phi'_1 s} + \mathcal{K}_{2,j} e^{i\phi'_2 s}. \quad (11)$$

Equation (4) can be integrated across the j th card to obtain the difference equations:

$$\tilde{\xi}(s_{j+}) = \tilde{\xi}(s_{j-}), \quad (12)$$

$$\tilde{\xi}'(s_{j+}) - \tilde{\xi}'(s_{j-}) = \mathcal{I}_c \tilde{\xi}(s_j). \quad (13)$$

The negative sign denotes the side of the yaw card that the projectile approaches and the plus sign denotes the side of the card that the projectile leaves. Equations (12) and (13)

show that the value of the epicyclic yaw is not changed by the projectile-card interaction, but the derivative of yaw is changed.

3.1 Modal Parameters Before and After Interaction

Equation (11) and its derivative with respect to s can be substituted into the difference equations and solved for $\mathcal{K}_{k,j+1}$ in terms of $\mathcal{K}_{k,j}$, in which $k = 1, 2$ and j can also have the value zero:

$$\mathcal{K}_{1,j+1} = \mathcal{K}_{1,j} - \frac{i\mathcal{I}_c}{\phi'_1 - \phi'_2} \mathcal{K}_{1,j} - \frac{i\mathcal{I}_c}{\phi'_1 - \phi'_2} \mathcal{K}_{2,j} e^{-i(\phi'_1 - \phi'_2)s_{j+1}}, \quad (14)$$

$$\mathcal{K}_{2,j+1} = \mathcal{K}_{2,j} + \frac{i\mathcal{I}_c}{\phi'_1 - \phi'_2} \mathcal{K}_{2,j} + \frac{i\mathcal{I}_c}{\phi'_1 - \phi'_2} \mathcal{K}_{1,j} e^{i(\phi'_1 - \phi'_2)s_{j+1}}. \quad (15)$$

Cooper & Fansler (1997) defined

$$\begin{aligned} \mu &\equiv \frac{\mathcal{I}_c}{\phi'_1 - \phi'_2} \\ &= \frac{\mathcal{I}_c}{\sqrt{P^2 - 4M}}, \end{aligned} \quad (16)$$

$$\begin{aligned} S_j &\equiv (\phi'_1 - \phi'_2)s_j \\ &= \sqrt{P^2 - 4M}s_j, \end{aligned} \quad (17)$$

so that,

$$\mathcal{K}_{1,j+1} = \mathcal{K}_{1,j} - i\mu\mathcal{K}_{1,j} - i\mu\mathcal{K}_{2,j}e^{-iS_{j+1}}, \quad (18)$$

$$\mathcal{K}_{2,j+1} = \mathcal{K}_{2,j} + i\mu\mathcal{K}_{2,j} + i\mu\mathcal{K}_{1,j}e^{iS_{j+1}}, \quad (19)$$

in which μ is called the impact stability parameter. Equations (18) and (19) were used to obtain the point-by-point results and the approximation that delineated the line between stable and unstable flight behavior (Cooper & Fansler 1997).

The square of the moduli of $\mathcal{K}_{1,j+1}$ and $\mathcal{K}_{2,j+1}$ can be immediately obtained from Equations (18) and (19).

$$\begin{aligned} \left(\frac{K_{1,j+1}}{K_{1,j}}\right)^2 &= 1 - 2\mu\frac{K_{2,j}}{K_{1,j}}\sin(\Phi_{j+1}) + \\ &\mu^2\left[1 + \left(\frac{K_{2,j}}{K_{1,j}}\right)^2 + 2\frac{K_{2,j}}{K_{1,j}}\cos(\Phi_{j+1})\right], \end{aligned} \quad (20)$$

$$\begin{aligned} \left(\frac{K_{2,j+1}}{K_{2,j}}\right)^2 &= 1 - 2\mu\frac{K_{1,j}}{K_{2,j}}\sin(\Phi_{j+1}) + \\ &\mu^2\left[1 + \left(\frac{K_{1,j}}{K_{2,j}}\right)^2 + 2\frac{K_{1,j}}{K_{2,j}}\cos(\Phi_{j+1})\right], \end{aligned} \quad (21)$$

in which

$$\Phi_{j+1} \equiv S_{j+1} + \hat{\phi}_j, \quad (22)$$

in which

$$\hat{\phi}_j \equiv \phi_{1,j} - \phi_{2,j}, \quad (23)$$

and Φ_{j+1} is called the epicyclic phase encounter value at the j th + 1 card.

The explicit expression for the sine of the modal arm phase angle change at each yaw card, which was obtained earlier (Cooper & Fansler 1997), is

$$\sin(\phi_{1,j+1} - \phi_{1,j}) = \frac{-\mu[K_{1,j} + K_{2,j} \cos(\Phi_{j+1})]}{K_{1,j+1}}, \quad (24)$$

$$\sin(\phi_{2,j+1} - \phi_{2,j}) = \frac{\mu[K_{2,j} + K_{1,j} \cos(\Phi_{j+1})]}{K_{2,j+1}}. \quad (25)$$

For $K_{1,j} = K_{2,j}$, Equations (24) and (25) show that the card-modified phase angle, $\phi_{1,j}$, of the fast arm is always reduced by the impact, while the card-modified phase angle, $\phi_{2,j}$, of the slow modal arm is always advanced. The total epicyclic phase change caused by the impact would be $\hat{\phi}_{j+1} - \hat{\phi}_j$. The epicyclic phase jump is defined as

$$\sigma_{j+1} \equiv -(\hat{\phi}_{j+1} - \hat{\phi}_j), \quad (26)$$

Figure 1 shows the epicyclic phase jump, σ_{j+1} , and the modal amplitude change induced by the interaction normalized by their maximum values as a function of the epicyclic encounter value, Φ_{j+1} .

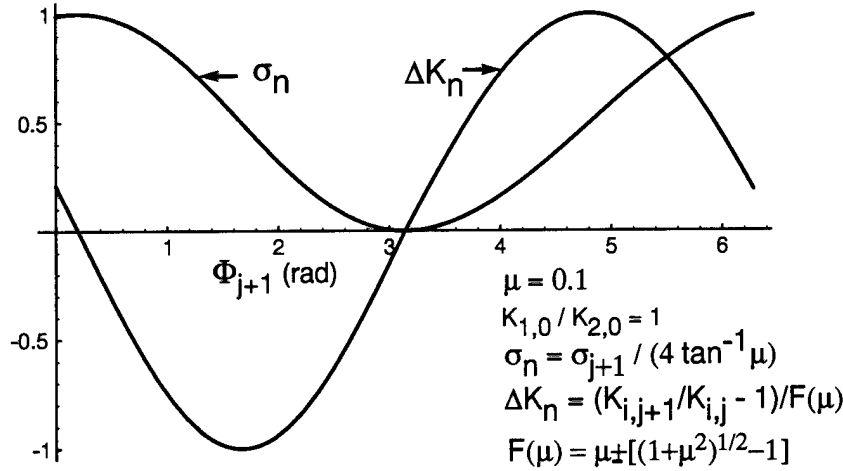


Figure 1. Normalized Phase Jump and Modal Arm Amplitude Versus the Epicyclic Phase Encounter Value ($\mu = 0.1$).

The maximum value of σ_{j+1} can be easily obtained from Equation (25) with the assumption that $\sigma_{j+1}/2 = \phi_{2,j+1} - \phi_{2,j}$. Differentiation of Equation (25) with respect to the encounter

phase value and setting the expression equal to zero will, with trigonometric identities, yield the maximum value, $\sigma_{j+1} = 4 \tan^{-1} \mu$, which is used to normalize Φ_{j+1} in Figure 1.

Also superimposed upon the figure is the normalized curve for the fractional increase or decrease in the modal arm amplitude. The phase encounters resulting in decreasing modal arms, $\Delta K_n < 0$, occur for $2 \tan^{-1} \mu < \Phi_{j+1} < \pi$, while the phase encounters that yield only increasing modal arm amplitudes occur for the values, $\pi < \Phi_{j+1} < 2\pi + 2 \tan^{-1} \mu$. These boundary points, or points where $\Delta K_n = 0$, can immediately be obtained by setting the amplitude ratios in Equations (20) and (21) to one and solving for the phase encounter values. The minimum and maximum values of ΔK_n occur when $\Phi_{j+1} = \pi/2 + \tan^{-1} \mu$ and $\Phi = 3\pi/2 + \tan^{-1} \mu$, respectively. These extreme values can be obtained by differentiating Equations (20) and (21) with respect to the phase encounter value and setting equal to zero and solving. The negative part of the curve showing the fractional decrease in the modal arm amplitudes is normalized by the value, $\mu - \sqrt{1 + \mu^2} + 1$, whereas the fractional increase in the modal arm amplitudes is normalized by $\mu + \sqrt{1 + \mu^2} - 1$. The interaction takes place $\tan^{-1} \mu$ past the points where the projectile is pitching most rapidly down and up, respectively. The interaction yields $\sigma_{j+1} = 2 \tan^{-1} \mu$ with the interaction effectively taking place around minimum and maximum values of $d|\tilde{\xi}|/ds$. The force that occurs on the projectile at these values is along the lateral motion of the projectile. This is an example of the general result that a given impulse changes the kinetic energy maximally when the absolute value of the dot product of the momentum with the impulse is a maximum.

An invariant relation between the magnitudes of the two modal arms is applicable to both stable and unstable yawing motion. Some manipulation of Equations (20) and (21) yields

$$K_{1,j+1}^2 - K_{2,j+1}^2 = K_{1,j}^2 - K_{2,j}^2. \quad (27)$$

The above equation then implies that

$$K_{1,j}^2 - K_{2,j}^2 = K_{1,0}^2 - K_{2,0}^2, \quad (28)$$

which is a hyperbola curve in two-dimensional space for the two modal arms, which expresses an invariant quantity for the interaction process.

3.2 Solution for Uniform Yaw Card Range With Difference Equations

Equations (20), (21), (24), and (25) can be used to obtain a point-by-point calculation of the modal behavior for cards with any arbitrary spacing, but yaw card ranges are usually comprised of a series of equally spaced cards to facilitate obtaining the projectile's flight coefficients. If the intervals between the cards are all equal, the phase interval characterizing

the range is

$$\gamma_o \equiv S_{j+1} - S_j, \quad (29)$$

a relationship between the yaw arms for three succeeding cards can be obtained:

$$\mathcal{K}_{1,j+2} - 2ge^{-i\gamma/2}\mathcal{K}_{1,j+1} + e^{-i\gamma}\mathcal{K}_{1,j} = 0, \quad (30)$$

$$\mathcal{K}_{2,j+2} - 2ge^{i\gamma/2}\mathcal{K}_{2,j+1} + e^{i\gamma}\mathcal{K}_{2,j} = 0, \quad (31)$$

in which

$$\gamma \equiv \gamma_o - 2m\pi, \quad (32)$$

$$g \equiv \mu \sin(\gamma/2) + \cos(\gamma/2). \quad (33)$$

in which $m = 0$ or a positive integer and $0 \leq \gamma < 2\pi$. When $m \geq 1$, the cards are spaced so far apart that more than one cycle of motion occurs. The symbol, γ , will be called the principal phase interval. The use of the principal phase interval simplifies the analysis and equations. It is assumed that the values of $\phi_{1,0}$ and $\phi_{2,0}$ are the initial phase values of the fast and slow modal arms, respectively, found at a phase interval, γ_o , in front of the first card.

To solve the difference Equations (30) and (31), define

$$\mathcal{K}_{1,j} \equiv \mathcal{Q}_{1,j}e^{-i\gamma j/2}, \quad (34)$$

$$\mathcal{K}_{2,j} \equiv \mathcal{Q}_{2,j}e^{i\gamma j/2}. \quad (35)$$

Equations (30) and (31) then become

$$\mathcal{Q}_{1,j+2} - 2g\mathcal{Q}_{1,j+1} + \mathcal{Q}_{1,j} = 0, \quad (36)$$

$$\mathcal{Q}_{2,j+2} - 2g\mathcal{Q}_{2,j+1} + \mathcal{Q}_{2,j} = 0, \quad (37)$$

which are in a standard form (Hildebrand 1968). In the above form, Equations (36) and (37) are equivalent and have the same general solution. Another standard form, which may be more convenient to work with, is provided by substitution with the definitions:

$$\cos \theta \equiv g \text{ for } g < 1, \quad (38)$$

$$\cosh \theta \equiv g \text{ for } g > 1. \quad (39)$$

When $g < 1$, the difference equations yield stable solutions, whereas when $g \geq 1$, unstable solutions are obtained (Hildebrand 1968). For $g < 1$, the general solution to Equations (36) and (37) is, using the above definitions,

$$\mathcal{Q}_{1,j} = A_{1,1} \sin(j-1)\theta + A_{1,2} \sin j\theta, \quad (40)$$

$$\mathcal{Q}_{2,j} = A_{2,1} \sin(j-1)\theta + A_{2,2} \sin j\theta. \quad (41)$$

For $g > 1$, substitute $i\theta$ for θ to obtain the hyperbolic functions.

Substitution of Equations (40) and (41) into Equations (36) and (37) with $j = 0$ and $j = 1$ gives the expression for the modal complex yaw arm and yields for $g < 1$, in terms of the initial conditions:

$$\mathcal{K}_{1,j} = \frac{e^{-i\gamma(j-1)/2}}{\sin \theta} \{[\mathcal{K}_{1,0}(1 - i\mu) - i\mu\mathcal{K}_{2,0}e^{-i\gamma}] \sin j\theta - \mathcal{K}_{1,0}e^{-i\gamma/2} \sin(j-1)\theta\}, \quad (42)$$

$$\mathcal{K}_{2,j} = \frac{e^{i\gamma(j-1)/2}}{\sin \theta} \{[\mathcal{K}_{2,0}(1 + i\mu) + i\mu\mathcal{K}_{1,0}e^{i\gamma}] \sin j\theta - \mathcal{K}_{2,0}e^{i\gamma/2} \sin(j-1)\theta\}, \quad (43)$$

The quantities within the square brackets in the above equations are the values of the modal arms after passing through the first card. Again, for $g > 1$, the above trigonometric functions are replaced by the respective hyperbolic functions:

$$\mathcal{K}_{1,j} = \frac{e^{-i\gamma(j-1)/2}}{\sinh \theta} \{[\mathcal{K}_{1,0}(1 - i\mu) - i\mu\mathcal{K}_{2,0}e^{-i\gamma}] \sinh j\theta - \mathcal{K}_{1,0}e^{-i\gamma/2} \sinh(j-1)\theta\}, \quad (44)$$

$$\mathcal{K}_{2,j} = \frac{e^{i\gamma(j-1)/2}}{\sinh \theta} \{[\mathcal{K}_{2,0}(1 + i\mu) + i\mu\mathcal{K}_{1,0}e^{i\gamma}] \sinh j\theta - \mathcal{K}_{2,0}e^{i\gamma/2} \sinh(j-1)\theta\}, \quad (45)$$

The ratios of the j th yaw arm moduli to their original values can be obtained either from first principles or with algebraic manipulation of Equations (42) and (43), with substitution for trigonometric identities. The resulting equations are, for $g < 1$,

$$\left(\frac{K_{1,j}}{K_{1,0}}\right)^2 - 1 = \frac{\sin j\theta}{\sin^2 \theta} [\mathcal{C}_1 \sin j\theta + \mathcal{D}_1 \sin(j-1)\theta], \quad (46)$$

$$\left(\frac{K_{2,j}}{K_{2,0}}\right)^2 - 1 = \frac{\sin j\theta}{\sin^2 \theta} [\mathcal{C}_2 \sin j\theta + \mathcal{D}_2 \sin(j-1)\theta], \quad (47)$$

in which, the constants, \mathcal{C}_1 , \mathcal{C}_2 , \mathcal{D}_1 , and \mathcal{D}_2 are

$$\mathcal{C}_1 = -2\mu \frac{K_{2,0}}{K_{1,0}} \sin \hat{\Phi}_1 + \mu^2 \left[1 + \left(\frac{K_{2,0}}{K_{1,0}}\right)^2 + 2\frac{K_{2,0}}{K_{1,0}} \cos \hat{\Phi}_1 \right], \quad (48)$$

$$\mathcal{C}_2 = -2\mu \frac{K_{1,0}}{K_{2,0}} \sin \hat{\Phi}_1 + \mu^2 \left[1 + \left(\frac{K_{1,0}}{K_{2,0}}\right)^2 + 2\frac{K_{1,0}}{K_{2,0}} \cos \hat{\Phi}_1 \right], \quad (49)$$

$$\mathcal{D}_1 = 2\mu \frac{K_{2,0}}{K_{1,0}} \sin(\hat{\Phi}_1 - \gamma/2), \quad (50)$$

$$\mathcal{D}_2 = 2\mu \frac{K_{1,0}}{K_{2,0}} \sin(\hat{\Phi}_1 - \gamma/2), \quad (51)$$

in which

$$\hat{\Phi}_1 \equiv \gamma + \phi_{1,0} - \phi_{2,0}. \quad (52)$$

Since $\hat{\Phi}_1$ corresponds to the initial conditions at the first card, the initial starting condition can be relaxed to any position in front of the first card and $\hat{\Phi}_1$ can be replaced by Φ_1 , as in Equation (22), in which

$$\Phi_1 \equiv S_1 + \hat{\phi}_o. \quad (53)$$

From Equations (20) and (21), the values \mathcal{C}_1 and \mathcal{C}_2 are recognized as the square of the moduli minus 1.

For unstable yawing motion, or equivalently, $g > 1$, substitute the hyperbolic functions for the trigonometric functions wherever the function argument is θ . With further manipulation, the expression can be written as an increasing term plus a decreasing term minus a constant value term:

$$\left(\frac{K_{1,j}}{K_{1,0}}\right)^2 - 1 = \frac{(\mathcal{C}_1 + \mathcal{D}_1 e^{-\theta}) e^{2j\theta} + (\mathcal{C}_1 + \mathcal{D}_1 e^{\theta}) e^{-2j\theta} - 2(\mathcal{C}_1 + \mathcal{D}_1 \cosh \theta)}{4 \sinh^2 \theta}, \quad (54)$$

$$\left(\frac{K_{2,j}}{K_{2,0}}\right)^2 - 1 = \frac{(\mathcal{C}_2 + \mathcal{D}_2 e^{-\theta}) e^{2j\theta} + (\mathcal{C}_2 + \mathcal{D}_2 e^{\theta}) e^{-2j\theta} - 2(\mathcal{C}_2 + \mathcal{D}_2 \cosh \theta)}{4 \sinh^2 \theta}. \quad (55)$$

For $g = 1$, the general solution for the squared amplitude of the modal arms can be obtained by taking the limit of θ going to zero in Equations (46) and (47):

$$\left(\frac{K_{1,j}}{K_{1,0}}\right)^2 - 1 = j[(\mathcal{C}_1 + \mathcal{D}_1)j - \mathcal{D}_1], \quad (56)$$

$$\left(\frac{K_{2,j}}{K_{2,0}}\right)^2 - 1 = j[(\mathcal{C}_2 + \mathcal{D}_2)j - \mathcal{D}_2], \quad (57)$$

Although the projectile flight is unstable for $g = 1$, the modal arm amplitudes increase only linearly instead of exponentially, as occurs for $g > 1$.

For stable yawing motion, Cooper and Fansler (1997) observed that the values for the change from the initial modal lengths lay in an envelope with a midpoint average value that was, in general, not zero. If Equations (46) and (47) are integrated with j treated as a variable and then divided by the integrated interval, the average values are found to be

$$\overline{\left(\frac{K_{1,j}}{K_{1,0}}\right)^2 - 1} = \frac{1}{2 \sin^2 \theta} [\mathcal{C}_1 + \mathcal{D}_1 \cos \theta], \quad (58)$$

$$\overline{\left(\frac{K_{2,j}}{K_{2,0}}\right)^2 - 1} = \frac{1}{2 \sin^2 \theta} [\mathcal{C}_2 + \mathcal{D}_2 \cos \theta]. \quad (59)$$

Here the average value depends both on the initial modal phase and the card interval spacing. As γ is varied so that the stability boundary is approached, then $\sin \theta$ becomes smaller and the absolute values of the average quantities can become larger.

4. STABILITY BOUNDARIES AND GROWTH IN YAW

In the last section, it was shown that the boundary for stability corresponded to the condition that $g = 1$. With trigonometric identities, it can be established from the definition

for g , Equation (33), that the stability boundaries for γ_o encompassing phase difference intervals are given by

$$\gamma_{\text{low}} = 2m\pi, \quad (60)$$

$$\gamma_{\text{high}} = 2m\pi + 4 \tan^{-1} \mu, \quad (61)$$

in which $m = 0$ or a positive integer and $K_{1,0} = K_{2,0}$. The usual approximate launch condition from an unworn gun is $K_{1,0}/K_{2,0} = 1$. The subscripts “low” and “high” designate the minimum and maximum values of the phase interval for a given region designated by the integer, m .

The maximum growth curves in the μ, γ_o -plane are obtained by differentiation of Equation (33) with respect to γ and setting the resulting expression equal to zero:

$$\gamma_{\text{max}} = 2m\pi + 2 \tan^{-1} \mu. \quad (62)$$

in which $K_{1,0} = K_{2,0}$. Figure 2 shows the first two of the regions for stable and unstable behavior. The growth rate is a maximum when $\gamma_o = 2 \tan^{-1} \mu$ for the lower unstable region and $\gamma_o = 2\pi + 2 \tan^{-1} \mu$ for the next unstable region. This maximum growth rate curve corresponds to $g = \sqrt{1 + \mu^2}$.

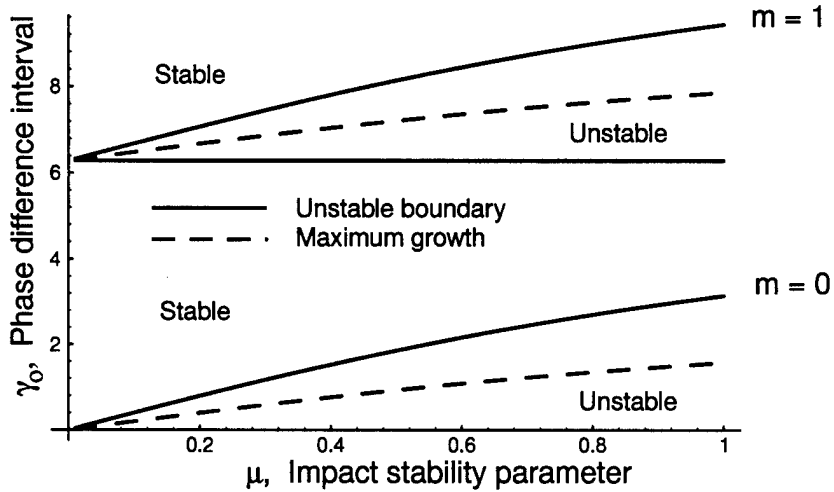


Figure 2. Stable and Unstable Regions as a Function of μ .

Cooper and Fansler (1997) have already shown that with some assumptions including $\mu \ll 1$, the condition for stability as given by McCoy (1992) can be reproduced. This condition can also be obtained with the present approach, assuming only that $\mu \ll 1$. The conditions for instability in the present approach are that $g \geq 1$ or, equivalently,

$$\mu \sin \frac{\gamma}{2} + \cos \frac{\gamma}{2} \geq 1. \quad (63)$$

Expand the trigonometric functions in series for small γ . For limiting small values of μ , only the first terms need to be kept to obtain the conditions for instability:

$$\mu - \gamma/4 \geq 0. \quad (64)$$

With Equations (29), (64), (16), (3), and (2), and some algebraic manipulation, the approximate gyroscopic stability factor for stable yawing motion is

$$S_g = \frac{P^2}{4(M + M_c \tau_c / d_c)} > 1. \quad (65)$$

The boundaries obtained for the approximation, Equation (64), and the exact solution are shown in Figure 3. Here, it is shown that the approximate solution agrees well for $\mu < 0.4$ and, for conventional yaw card ranges ($\mu = 0.1$ for a card range designed for a 7.62-mm rifle, according to McCoy [1992]), the approximate solution is adequate. For larger values of μ , the straight line approximation of γ by Equation (64) is larger than the exact value.

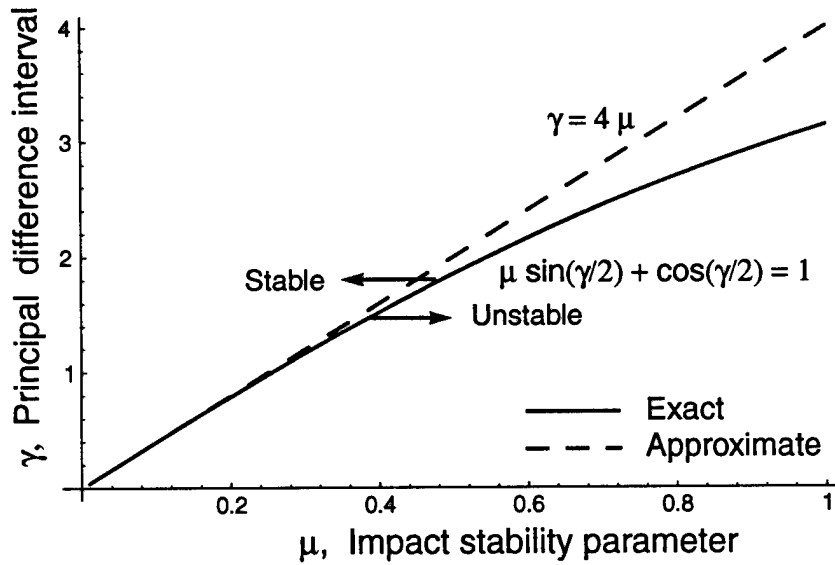


Figure 3. Comparison Between Approximate and Exact Solution for the Stability Boundary.

Some general conclusions can be obtained by examining the unstable behavior of the modal arms for a large number of yaw cards. To investigate the asymptotic behavior of card interactions, treat the card index number, j , as a continuous variable and differentiate Equation (44) with respect to j obtaining

$$\frac{d\mathcal{K}_{1,j}}{dj} \approx \left(\theta - \frac{i\gamma}{2}\right)\mathcal{K}_{1,j}. \quad (66)$$

Integrating Equation (66), it is obtained that for a card index value, k , larger than j the

value for the first modal arm is approximately

$$\mathcal{K}_{1,k} = e^{(k-j)\theta} e^{-i(k-j)\gamma/2} \mathcal{K}_{1,j}. \quad (67)$$

Equation(67) shows that, for large index card numbers, the magnitude of the modal arms will always increase and the phase change at each encounter is simply half the principal value of the phase difference interval. Likewise, the second modal arm amplitude will increase in the same way, but the second modal arm will be advanced instead of retarded. These results show that the behavior of the modal arms at large values of j is independent of the initial conditions. Note that no restrictions have been placed on the relative phases or sizes of the modal arms. Even though the initial phase encounter value may be such that the amplitudes of the modal yaw arms decline as the first part of the yaw card range is traversed, the phase encounter values eventually adjust so that the phase shift and amplification factor depend only on the stability parameter, μ , and the principal value of the phase difference interval, γ . For small values of μ , $\theta^2 \approx \gamma(\mu - \gamma/4)$ and $\theta^2 \approx 2(g - 1)$.

For large values of j , $K_{1,j+1} \approx K_{2,j+1}$, from Equation (28). With $K_{1,j+1}/K_{1,j}$ approaching a constant value, according to Equation (66), the epicyclic phase encounter value, Φ_{j+1} , also approaches an unchanged or stationary value, from Equations (20), (21), (24), and (25). This means that the epicyclic phase jump, σ_{j+1} , asymptotically approaches the phase interval value, γ , as the projectile advances through the range. The value of Φ_{j+1} would depend on the value of $\gamma \approx \sigma_{j+1}$, determined by the functional form shown in Figure 1.

The same functional form is obtained from the solution to the difference equation. Setting the second term in parentheses on the right-hand side in Equations (54) and (55) equal to zero and solving for the relationship between Φ_1 and γ gives the condition for stationary phase encounter values, $\Phi_{j+1} = \Phi_1$, that yield modal arm amplitudes with a constant factor for the increase. In the same manner, setting the first term in parentheses on the right-hand side in Equations (54) and (55) equal to zero and solving for the relationship between Φ_{j+1} and γ gives the condition for stationary phase encounter values that yield decreasing modal arm amplitudes. The value of Φ_1 that satisfies these conditions for a given value of γ is designated as Φ_γ . One value of Φ_γ would be found for both an increasing and a decreasing value for the change in the modal arm amplitude.

The solutions for γ_n are given in Figure 4, which shows the phase interval values as a function of Φ_n for $\mu = 0.1$. Equation (67) shows that the phase encounter values, $2 \tan^{-1} \mu < \Phi_{j+1} < \pi$, cannot exist for large values of j with cards uniformly spaced. The curve is shown as dashed wherever there is a fractional decrease. Because the phase encounter values cannot occur for large values of j when the amplitude is decreasing, these corresponding phase encounter values are more accurately designated as pseudo-stationary phase solutions or the

phase encounter solutions for the pseudo-stationary branch for the phase interval between yaw cards, γ_n .

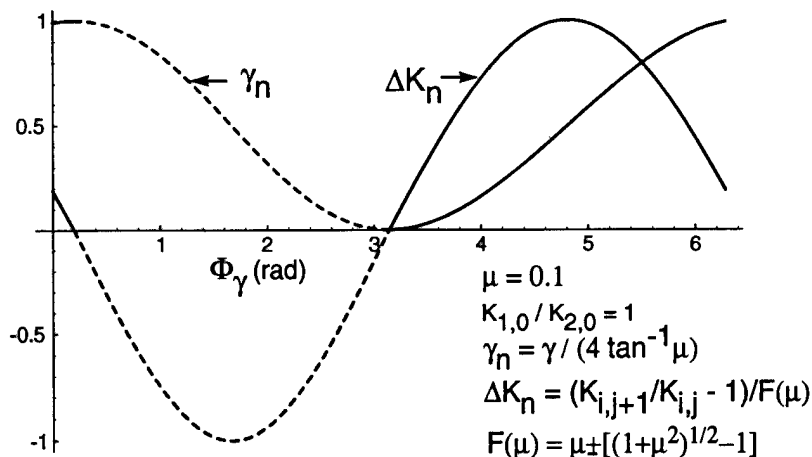


Figure 4. Stationary Phase Encounter Values Versus the Phase Interval with the Superimposed Curve for the Fractional Change in the Modal Arm Amplitudes ($\mu = 0.1$).

Much of the information about stationary phase solutions could also be obtained from the single card treatment of the preceding section. If one assumes that $\gamma = \sigma_{j+1}$, Figure 4 can be obtained, but with no immediate knowledge of the pseudo-stationary solutions. The value of γ is normalized by dividing by its maximum value, $4 \tan^{-1} \mu$, which occurs at $\Phi_{j+1} = 2 \tan^{-1} \mu$. Figure 4 shows that the modal arm amplitude remains constant at both $\Phi_{j+1} = 2 \tan^{-1} \mu$ and $\Phi_{j+1} = \pi$. The latter value corresponds to the position where the projectile is aligned with the flight direction (neglecting the yaw of repose), and minimal interaction with the target would be expected.

The expression in the second set of parentheses in Equation (54), when set equal to zero to obtain stationary encounter phase solutions, can be used to obtain a relationship between a shifted value of the encounter phase value and the phase interval between cards. The expression in the first set of parentheses could also be used because the modal arms are assumed equal, and a squaring operation will be used that enables applicability to both decreasing and increasing values of the modal arms. When the resulting equation is expressed in terms of $\Phi_\gamma - \gamma/2$ and the results squared to obtain a quadratic equation that is solved, a transcendental relationship is obtained between the transformed value of the encounter phase and phase interval between cards:

$$\cos \bar{\Phi}_\gamma = \frac{\sin(\gamma/2)}{\mu} - \cos(\gamma/2). \quad (68)$$

With the substitution of $\tan a$ for μ and using trigonometric identities, Equation (68) can

be represented as

$$\cos \bar{\Phi}_\gamma = \frac{\sin(\gamma/2 - a)}{\sin a}, \quad (69)$$

in which $a = \tan^{-1} \mu$. Both the quantities, $\gamma/2 - a$ and a , in Equation (69) are small enough so that they can well approximate their sine functions. Finally, dividing γ by the normalizing factor, $4 \tan^{-1} \mu$, yields the quasi-universal relationship between the normalized value of γ and $\bar{\Phi}_\gamma$:

$$\gamma_n \approx (1 + \cos \bar{\Phi}_1)/2, \quad (70)$$

in which $\bar{\Phi}_\gamma \equiv \Phi_\gamma - \gamma/2$ which applies for all realistic values of μ for a yaw card range. By transforming to the variable, $\bar{\Phi}_\gamma$, the relationship between the phase interval difference, γ , for the card spacing and the value of $\bar{\Phi}_\gamma$ needed to maintain a constant value of the epicyclic phase encounter value, Φ_{j+1} , at the arbitrary j th + 1 card is given by Equation (70).

Comparison with Equation (68) for the exact value and the approximate expression, Equation (70), shows that the error in the approximation is less than 0.3% for $\mu = 0.3$ and for the transformed values at $\bar{\Phi}_1 \approx m\pi/4$, where the most error occurs with odd integer values of m . By expansion into series form, it can be shown that the error condition when using the above approximation is

$$\text{Error} < \mu^2 \sin(2\bar{\Phi}_1)(\sin \bar{\Phi}_1)/24. \quad (71)$$

The approximation, Equation (70), becomes exact where $\bar{\Phi}_1 = m\pi/2$, in which m equals an integer with zero included.

Equation (70) has far-reaching consequences for isolated encounters of a projectile with a yaw card. Since $\sigma_{j+1} = \gamma$ when the condition of a constant phase encounter value is achieved and the card encounter phase, Φ_{j+1} , determines the value of phase encounter jump, σ_{j+1} , it is deduced that

$$\sigma_{j+1} \approx 2(\tan^{-1} \mu)(1 + \cos \bar{\Phi}_{j+1}), \quad (72)$$

in which $\bar{\Phi}_{j+1} \equiv \Phi_{j+1} - \sigma_{j+1}/2$ for an arbitrary yaw card. The transformed phase encounter value, $\bar{\Phi}_{j+1}$, may be interpreted as the center point of the encounter phase value around which the interaction takes place. Immediately after the interaction, the phase encounter value is reduced to $\Phi_{j+1} - \sigma_{j+1}$.

Figure 5 shows the normalized value of the phase jump, σ_n , for $\mu = 0.05$ and $\mu = 0.3$, plotted as a function of the transformed phase encounter value, $\bar{\Phi}_{j+1}$. These values of the stability parameter range from one of the smaller values to one of the larger values of μ that might be encountered. The special case for stationary card encounter phase through a uniformly spaced range is also described by the results of Figure 5, in which $\gamma_n = \sigma_n$. The

differences in the values of σ_n plotted for the two different values of the stability parameter, μ , cannot be seen.

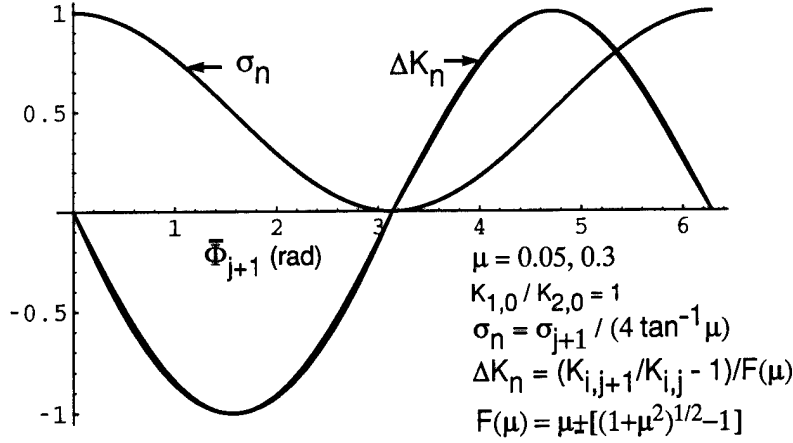


Figure 5. Normalized Phase Jump and Modal Amplitude Change Versus Quasi-Universal Transformed Card Encounter Phase Value.

Also shown is the fractional change in the modal arm amplitude, which is plotted for the stability parameters, $\mu = 0.05$ and $\mu = 0.3$. The plotted curves for ΔK_n show more differences than the curves for γ_n . These curves can be directly plotted by expressing Equation (20) in terms of the variable, $\bar{\Phi}_{j+1}$:

$$\left(\frac{K_{1,j+1}}{K_{1,j}} \right)^2 = 1 - 2g\mu \sin \bar{\Phi}_{j+1} + 2\mu^2 \sin^2 \bar{\Phi}_{j+1}. \quad (73)$$

Equation (72) not only represents a simple physical basis for the encounter phase and the epicyclic phase jump but can also be used, because of its fundamental functional form, to derive a simple expression for the phase encounter value, $\bar{\Phi}_{j+1}$, and to show how it approaches the stationary phase encounter value, $\bar{\Phi}_\gamma$, which depends on γ . For nonstationary phase encounter values, $\bar{\Phi}_{j+2}$ is simply the sum of the encounter phase at the j th + 1 card plus the interval phase, γ , traveled minus the phase jump, σ_{j+1} , from encountering the j th + 1 card:

$$\bar{\Phi}_{j+2} = \bar{\Phi}_{j+1} + \gamma - \sigma_{j+1}. \quad (74)$$

The behavior of the transformed phase encounter value with card index number can be obtained by first substituting in the right-hand side of Equation (74) with the results of Equations (70) and (72) to obtain

$$\bar{\Phi}_{j+2} - \bar{\Phi}_{j+1} = 2(\tan^{-1} \mu)(\cos \bar{\Phi}_\gamma - \cos \bar{\Phi}_{j+1}). \quad (75)$$

If the phase encounter value, $\bar{\Phi}_{j+1}$, corresponds to a value in the psuedo-stationary region, Equation (75) dictates that the value of the next encounter phase moves away from the value

of the encounter phase on the pseudo-stationary branch corresponding to γ and toward the encounter phase corresponding to γ on the stationary branch. Thus, $\bar{\Phi}_\gamma$ is the solution for the stationary phase encounter value, which is restricted to $\pi < \bar{\Phi}_\gamma < 2\pi$. Now for small values of μ , the approximation, $\bar{\Phi}_{j+2} - \bar{\Phi}_{j+1} \approx \Phi_{j+2} - \Phi_{j+1}$, and treat j as a continuous variable to obtain a differential equation whose solution is

$$\bar{\Phi}_{j+1} = 2 \tan^{-1} \frac{|\tan \frac{\bar{\Phi}_\gamma}{2}| \left[\tan \frac{\bar{\Phi}_1}{2} - |\tan \frac{\bar{\Phi}_\gamma}{2}| \tanh(j |\sin \bar{\Phi}_1| \tan^{-1} \mu) \right]}{\left[|\tan \frac{\bar{\Phi}_\gamma}{2}| - \tan \frac{\bar{\Phi}_1}{2} \tanh(j |\sin \bar{\Phi}_1| \tan^{-1} \mu) \right]}, \quad (76)$$

in which $\bar{\Phi}_1$ is the initial value for the transformed encounter phase and j assumes the value zero and any positive integer. Except for the singular point at $\pi/2$, Equation (76) shows that the asymptotic value for the transformed phase encounter value is always negative, which is equivalent to the asymptotic phase value being between π and 2π . These results are consistent with Equation (67), which shows that the phase jump approaches a constant value and that $K_{1,j+1}/K_{1,j} > 1$ for large values of j .

The epicyclic phase at card encounter as a function of the card index number is shown in Figure 6. The epicyclic phase at encounter with a yaw card was calculated point by point from the first card onward (Cooper & Fansler 1997) and also calculated with the approximation solution given by Equation (76). Comparisons between exact and approximate calculations showed no significant differences. The foregoing discussion describes the phase encounter values when the modal arms are equal. An expression has been obtained for unequal arms but is not given here because of its extreme complexity, which limits insight.

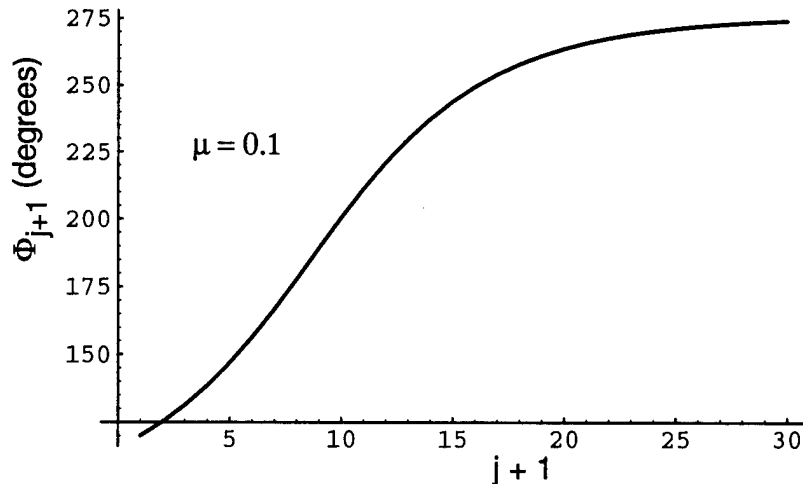


Figure 6. Phase Encounter Value Versus Card Index Number.

5. FURTHER DISCUSSION AND ILLUSTRATIONS

The equations developed are used to examine the detailed yawing motion of the projectile through a yaw card range. The equations giving the yaw arm values for each interval, Equations (42) and (43), are substituted into Equation (5) and plotted. The first example shows the yawing motion for a 7.62-mm projectile passing through a dense yaw card range discussed previously (McCoy 1992; Cooper & Fansler 1997). Figure 7 shows the yawing motion comparison of a projectile passing through 10 cards with one set of cards having $\mu = 0.1$ while the other set has another projectile passing through cards having $\mu = 0.0$. Having cards with $\mu = 0.0$ is an artifice that enables tracking the trajectory even though no cards exist in the range.

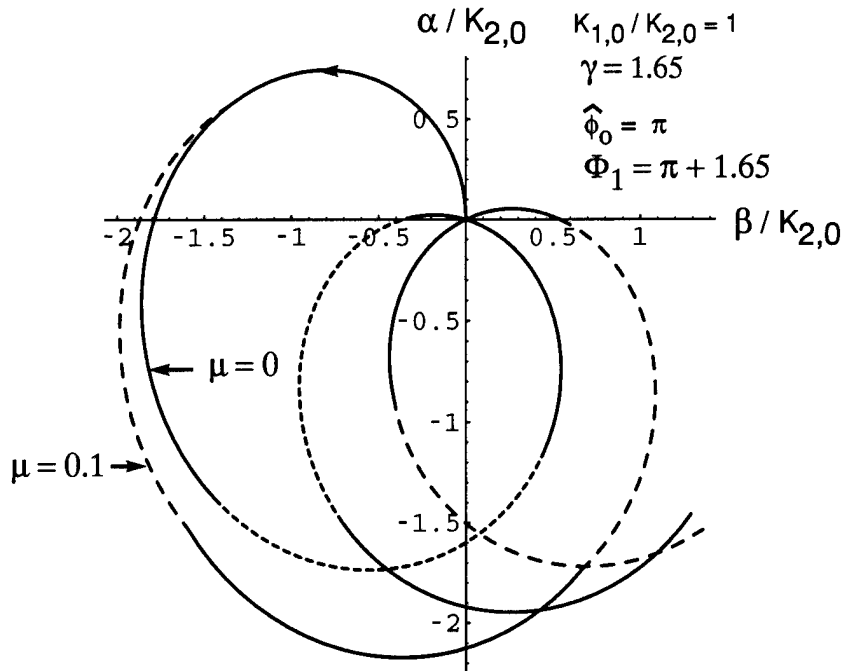


Figure 7. Comparisons of Stable Epicyclic Motion for the 7.62-mm Projectile.

The fast arm and slow arm are initially equal in length, which is approximately the initial conditions for many projectiles. The curves begin at the origin with $\phi_{1,0} = 2\pi$ and $\phi_{2,0} = \pi$, which yields for the initial value for the epicyclic yaw, $\hat{\phi}_0 = \pi$. The projectiles travel a phase distance, S_1 , equal to the phase interval, $\gamma = 1.65$, so that $\Phi_1 = 1.65 + \pi$. The phase encounter value at the first card plus the parameter values given in the figure completely define the motion. After each impact, the curves alternate between dashed and continuous lines. The

curves pass through the origin on each epicycle, because $K_{1,j} = K_{2,j}$ from Equation (28) when $K_{1,0} = K_{2,0}$.

Figure 8 shows the fast arm modal amplitude increasing by the maximum amount with each card encounter. The projectile encounters every card with the phase encounter value $\Phi_1 = (4m + 3)\pi/2 + \tan^{-1} \mu$. For this phase encounter value, $\sigma_{j+1} = 2 \tan^{-1} \mu$, and the principal phase interval must be such that $\gamma = 2 \tan^{-1} \mu$ to obtain maximal amplification.

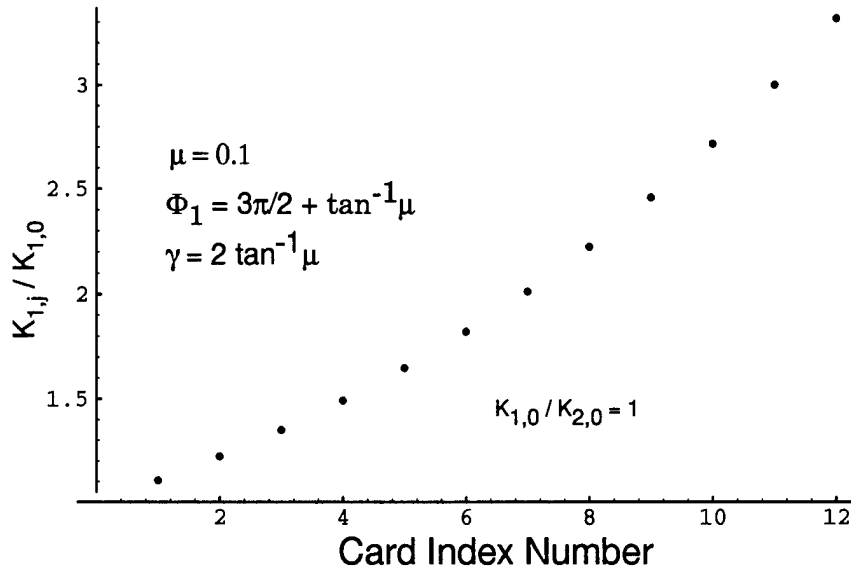


Figure 8. Maximum Growth of Fast Modal Arm.

Figure 9 shows the fast arm modal amplitude changing with maximal decay for each card encounter. The projectile encounters every card with the phase value $\Phi_{j+1} = (4m + 1)\pi/2 + \tan^{-1} \mu$. As discussed before, because $\sigma_{j+1} = 2 \tan^{-1} \mu$ for each encounter, the spacing for the principal phase interval must be such that $\gamma = 2 \tan^{-1} \mu$ to obtain maximal diminishment of the fast modal arm amplitude. Thus, the same range can be used to obtain Figures 8 and 9. The modal arm decrease is shown for only 12 cards in Figure 9, but with the computer precision used for the calculation, the curve will start ascending if a hundred or more cards are traversed. The first terms in Equations (54) and (55) become large relative to the second terms for large enough values of j . The smaller the precision in the computer's approximation for the starting value or the principal phase interval, the sooner the curve ceases descending and starts evolving into an exponentially increasing curve. This behavior has its counterpart in solutions of linear differential equations with exponential solutions where the positive exponential term has a vanishing small initial component, which grows large for large values of the independent variable. In practice, it would be difficult to design an experiment that would yield the results shown in Figure 9. Substantial variations from

the initial value would result in a growing amplitude for the modal arms after traversing a few cards.

A card range designed to produce instability could be useful. For instance, high values of yaw could be induced by judicious placement of the yaw cards. The encounter phase values for the yaw cards can also be controlled with the yaw card range design. Cameras could be set up near the range exit to study the flow around the projectile at high angle of attack.

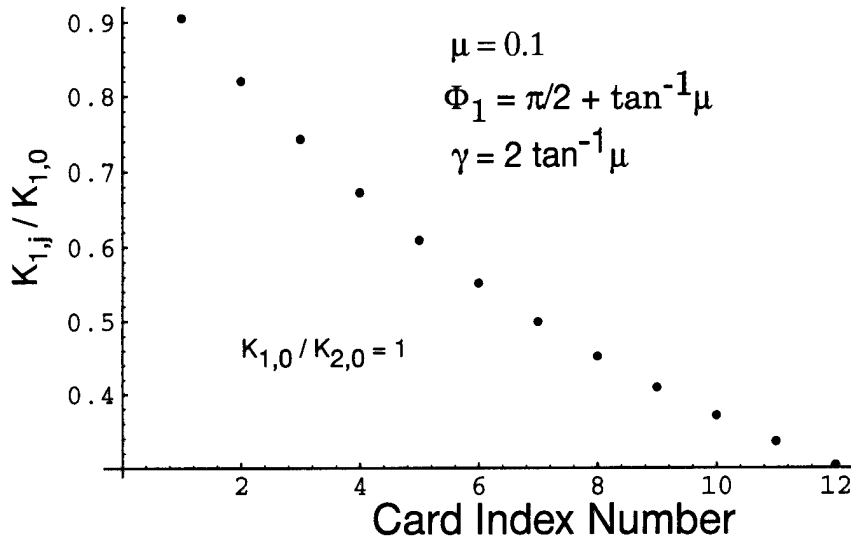


Figure 9. Maximum Decay of Fast Modal Arm Amplitude.

Figure 10 shows the detailed epicyclic yawing motion when the interval corresponds to the maximum value of g , which gives the maximum growth in yaw amplitude through a card range when the first encounter corresponds to the maximum yaw amplitude increase. Here, the starting condition is $\hat{\phi}_o = \pi$, and after traveling somewhat more than one epicycle, encounters the first card at $\Phi_1 = 3\pi + 2 \tan^{-1} \mu$. The yaw amplification at the first card will be very small because this phase value for the first encounter is very near to the encounter phase value for no amplification, $\Phi_1 = 3\pi$. Equations (24) and (25) show that the delay in the total phase value caused by the encounter with the first card is very small for $\mu = 0.1$. The interval value is larger than 2π and in subsequent card encounters, the encounter phase changes toward the value $\Phi_{j+1} = 2j\pi + 3\pi/2$, which corresponds to the maximum yaw amplification increase. The yawing motion passes through the origin because $K_{1,0} = K_{2,0}$. If the epicyclic arms had been unequal initially, the ratio of the arm lengths would have approached unity as the yaw card range was traversed. Then the point of closest approach to the origin for each epicycle would have been successively less as the yaw cards were traversed. For $\hat{\phi}_o = 2\pi$, the succeeding encounter phase values will again relax to the phase value that gives the maximum amplification. For any given initial phase value, with the

exception of $\Phi_1 = \pi/2$, the succeeding phase encounter values will relax toward the phase value that gives the maximum amplitude increase.

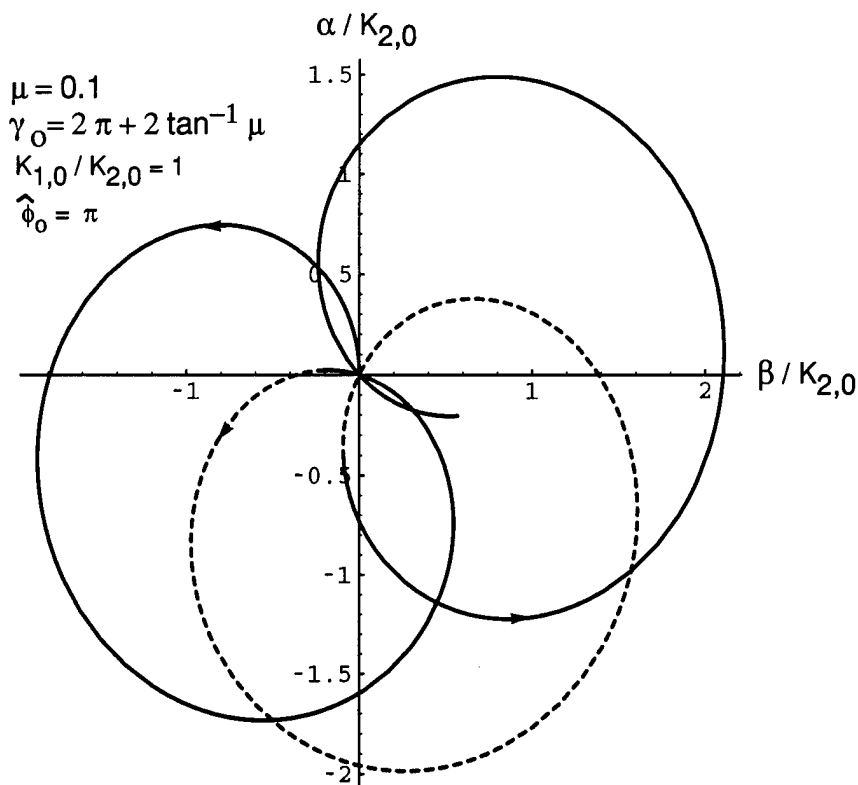


Figure 10. Unstable Epicyclic Motion for a 7.62-mm Projectile.

6. SUMMARY AND CONCLUSIONS

Stability and yaw growth for spin-stabilized projectiles passing through an array of equally spaced yaw cards are investigated. The encounters of the projectiles with the cards are treated as impulses, or mathematically, as Dirac delta functions. Solutions obtained by considering only one card yield expressions for modal arm amplitude changes and also phase changes that depend only upon the yaw card encounter phase value and the stability parameter.

The encounter with the yaw card retards the fast arm phase and accelerates the slow arm phase, resulting in a reduction of the epicyclic phase value. When the modal arm amplitudes are equal, these encounters equally retard and advance the fast arm phase and slow arm phase, respectively. These card-induced changes in modal arm phases result, for stable projectile flight, in a measured overturning moment that is larger than observed with

spark ranges.

For uniform yaw card arrays, the Dirac delta approach is used to develop difference equations for a three-card sequence. The difference equations have as parameters the phase interval between cards and a value that depends upon both the phase interval value and the stability parameter. The solution obtained describes the yaw arm phases and amplitudes as the projectile passes through the card array. It depends only on the phase encounter value for the first card, the phase interval between cards, and the stability parameter value. Stability boundaries are delineated and compared with approximate stability boundaries. Conditions for maximum yaw growth and decay with each card encounter are obtained.

If the intervals between yaw cards are such that the projectile experiences unstable flight, the encounter value for the projectile's epicyclic phase will asymptotically approach a value that depends only on the phase interval value between cards. This value is called the stationary encountered phase value for the yaw card range and can be readily calculated. A simple quasi-universal relationship between the stationary phase value and the card interval is further developed. A simple expression is also obtained for the epicyclic phase value that occurs at each card encounter as the projectile traverses the range for an arbitrary initial epicyclic phase encounter value.

7. REFERENCES

- McCoy, R. L. "The Effect of Yaw Cards on the Pitching and Yawing Motion of Symmetric Projectiles." U.S. Army Ballistic Research Laboratories BRL-TR-3338, Aberdeen Proving Ground, MD, May 1992 (AD 205633).
- Cooper, G. R. and K. S. Fansler. "Yaw Card Perturbation of Projectile Dynamics." U.S. Army Research Laboratory ARL-TR-1258, Aberdeen Proving Ground, MD 21005, January 1997.
- Dennerly, P. and A. Krzywicki. "*Mathematics for Physicists.*" Harper and Row, New York, 1967.
- Hildebrand, F. B.. "*Finite-Difference Equations and Simulations.*" Prentice-Hall, Inc., Englewood Cliffs NJ, 1968.
- Murphy, C. H. "Free Flight Motion of Symmetric Missiles." BRL-TR-1216, U.S. Army Ballistic Research Laboratories, Aberdeen Proving Ground, MD, May 1963 (AD 442757).

INTENTIONALLY LEFT BLANK.

LIST OF SYMBOLS

C_{M_α}	aerodynamic moment overturning coefficient
$C_{M_{\alpha c}}$	moment overturning coefficient for card material
d	projectile reference diameter
d_c	card spacing (m)
I_x	axial moment of inertia (kg-m ²)
I_y	transverse moment of inertia (kg-m ²)
\mathcal{I}_c	nondimensional overturning impulse for card material, $\frac{\rho_c A d^2 \tau_c}{2I_y} C_{M_{\alpha c}}$
j	card index value, $j = 0, 1, 2, \dots$
$K_{1,j}$	fast yaw mode magnitude after transit through j th yaw card
$K_{2,j}$	slow yaw mode magnitude after transit through j th yaw card
$\mathcal{K}_{1,j}$	$K_{1,j} \exp(i\phi_{1,j})$
$\mathcal{K}_{2,j}$	$K_{2,j} \exp(i\phi_{2,j})$
m	number of complete epicycles contained in interval, γ
M	nondimensionalized overturning moment, $\frac{\rho A d^3}{2I_y} C_{M_\alpha}$
M_c	nondimensionalized overturning moment for card material, $\frac{\rho_c A d^3}{2I_y} C_{M_{\alpha c}}$
$M_{(R)}$	apparent nondimensionalized overturning moment from card range
p	axial spin (rad/s)

P	$\frac{I_x p d}{I_y V}$
s	arc length along trajectory (calibers)
A	reference area, $\pi d^2/4$
S_g	gyroscopic stability factor
S_{j+1}	total phase distance to $j + 1$ card, $(\phi'_2 - \phi'_1)s_j$
V	magnitude of projectile velocity
α	angle of attack
α_t	total angle of attack
β	angle of side slip
γ_o	phase interval between uniformly space cards, $\gamma_o \equiv S_{j+1} - S_j$
γ	principal phase interval, $\gamma = \gamma_o - 2m\pi$, $0 < \gamma < 2\pi$
μ	impact stability parameter, $\frac{I_c}{\phi'_1 - \phi'_2}$
ρ	air density
ρ_c	density of card material (kg / m ³)
σ_{j+1}	jump of epicyclic phase caused by card encounter, $-(\hat{\phi}_{j+1} - \hat{\phi}_j)$
τ_c	card thickness (m)
$\phi_{1,j}$	fast mode phase angle, between j th and $j + 1$ card
$\phi_{2,j}$	slow mode phase angle, between j th and $j + 1$ card

$\hat{\phi}_j$	epicyclic phase value constant, $\phi_{1,j} - \phi_{2,j}$
ϕ'_1	fast mode angular velocity
ϕ'_2	slow mode angular velocity
Φ_{j+1}	epicyclic phase card encounter value, $S_{j+1} + \hat{\phi}_j$
$\bar{\Phi}_{j+1}$	transformed encounter phase value, $\Phi_{j+1} - \sigma_{j+1}/2$
$\bar{\Phi}_\gamma$	stationary transformed encounter phase value, $\Phi_{j+1} - \gamma/2$
$\tilde{\xi}$	$\sin \beta + i \sin \alpha$, complex yaw

INTENTIONALLY LEFT BLANK.

<u>NO. OF COPIES</u>	<u>ORGANIZATION</u>	<u>NO. OF COPIES</u>	<u>ORGANIZATION</u>
2	ADMINISTRATOR DEFENSE TECHNICAL INFO CENTER ATTN DTIC DDA 8725 JOHN J KINGMAN RD STE 0944 FT BELVOIR VA 22060-6218	2	COMMANDER U S ARMY TANK AUTOMOTIVE CMD ATTN AMCPM BFVS AMCPM BFVS SC K PITCO WARREN MI 48397-5000
1	DIRECTOR US ARMY RESEARCH LABORATORY ATTN AMSRL CS AL TA/RECORDS MGMT 2800 POWDER MILL ROAD ADELPHI MD 20783-1197	1	COMMANDER U S ARMY MISSILE COMMAND ATTN AMSMI RD DR W WALKER REDSTONE ARSENAL AL 35898-5000
1	DIRECTOR US ARMY RESEARCH LABORATORY ATTN AMSRL CI LL/TECH LIB 2800 POWDER MILL ROAD ADELPHI MD 20783-1197	1	COMMANDER TANK MAIN ARMAMENT SYSTEMS ATTN AMCPM TMA R BILLINGTON PICATINNY ARSENAL NJ 07806-5000
1	DIRECTOR US ARMY RESEARCH LABORATORY ATTN AMSRL CS AL TP/TECH PUB 2800 POWDER MILL ROAD ADELPHI MD 20783-1197	2	COMMANDANT U S ARMY INFANTRY SCHOOL ATTN ATSH IV SD R GORDAY ATSH TSM FORT BENNING GA 31905-5660
1	COMMANDER U S ARMY ARMAMENT MUNITIONS AND CHEMICAL COMMAND ATTN AMSMC LEP L ROCK ISLAND IL 61299-5000	3	DIRECTOR BENET LABORATORIES ATTN SMCAR CCB J BENDICK SMCAR CCB DS P VOTTIS SMCAR CCB RA WATERVLIET NY 12189-4050
1	DIRECTOR U S ARMY MISSILE & SPACE INTELLIGENCE CENTER ATTN AIAMS YDL REDSTONE ARSENAL AL 35898-5000	1	COMMANDER ARMY RESEARCH OFFICE ATTN AMXRO MCS MR K CLARK P O BOX 12211 RESEARCH TRIANGLE PARK NC 27709-2211
1	COMMANDER US ARMY ARMAMENT RD&E CENTER ATTN AMSTA AR TD MR HIRSHMAN PICATINNY ARSENAL NJ 07806-5000	1	COMMANDER ARMY RESEARCH OFFICE ATTN AMXRO RT IP LIBRARY SVS P O BOX 12211 RESEARCH TRIANGLE PARK NC 27709-2211
6	COMMANDER US ARMY ARMAMENT RD&E CENTER ATTN AMSTA AR AET A MR S KAHN MR M AMORUSO MR PEDERSEN MR C NG MR W TOLEDO MR B WONG PICATINNY ARSENAL NJ 07801-5000	1	COMMANDER AVIATION APPLIED TECHNICAL DIR ATTN SAVRT TY MSMA G MOFFATT PICATINNY ARSENAL NJ 07801-5000 FORT EUSTIS VA 23604-5577
1	COMMANDER US ARMY ARMAMENT RD&E CENTER ATTN AMSTA AR CCL D S LISS PICATINNY ARSENAL NJ 07801-5000		

<u>NO. OF COPIES</u>	<u>ORGANIZATION</u>	<u>NO. OF COPIES</u>	<u>ORGANIZATION</u>
3	DEPARTMENT OF THE ARMY CONSTRUCTION ENGINEERING RESEARCH LABORATORY ATTN CERL SOI P SCHOMER L PATER J WILCOSKI P O BOX 4000 CHAMPAIGN IL 61820	1	HONEYWELL COMPANY ATTN J GLASER S LANGLEY UNITED DEFENSE ARMAMENTS SYSTEM DIV 4800 EAST RIVER ROAD MINNEAPOLIS MN 55343
2	COMMANDER ASD/YHT ATTN WL/MNAA CPT J PALUMBO ASD/YHT D CURLEY EGLIN AFB FL 32542	1	S & D DYNAMICS INC ATTN R BECKER 7208 MONTRICO DR BOCA RATON FL 33433
1	COMMANDER (CODE 3433) NAVAL WARFARE CENTER ATTN TECH LIB CHINA LAKE CA 93555	1	AAI CORPORATION ATTN T STASNEY P O BOX 126 MS 100-405 HUNT VALLEY MD 21030-0126
2	COMMANDER NAVAL SURFACE WARFARE CENTER ATTN 6X J YAGLA G MOORE DAHLGREN VA 22448	2	AEROJET GENERAL CORPORATION ATTN W WOLTERMAN A FLATAU P O BOX 296 AZUSA CA 91702
1	COMMANDER (CODE 6120C) NAVAL ORDNANCE STATION ATTN SUSAN PETERS INDIAN HEAD MD 20640	2	LOCKHEED AIRCRAFT INC ATTN J BROWN J PEREZ PO BOX 33 DEPT 1-330/UPLAND ONTARIO CA 91761
1	COMMANDER (CODE 3892) NAVAL WARFARE CENTER ATTN K SCHADOW CHINA LAKE CA 93555	1	GENERAL ELECTRIC ARMAMENT & ELECTRIC SYSTEMS ATTN R WHYTE LAKESIDE AVENUE BURLINGTON VT 05401
1	COMMANDER (CODE 730) NAVAL SURFACE WARFARE CENTER SILVER SPRING MD 20910	1	FRANKLIN INSTITUTE ATTN TECH LIBRARY RACE & 20TH STREETS PHILADELPHIA PA 19103
1	DIRECTOR NASA SCIENTIFIC & TECHNICAL INFORMATION FACILITY ATTN SAK/DL PO BOX 8757 BALTIMORE/WASHINGTON INTERNATL AIRPORT MD 21240	1	THE JOHNS HOPKINS UNIV/CPIA 10630 LITTLE PATUXENT PARKWAY SUITE 202 COLUMBIA MD 21044-3200
1	MCDONNELL DOUGLAS ATTN JOSEPH SMUCKLER 1014 FERNGATE LANE CREVE COEUR MO 63141	2	LORAL CORPORATION ATTN S SCHMOTOLOCHA B AXELY 300 N HALSTEAD ST PO BOX 7101 PASADENA CA 91109

<u>NO. OF COPIES</u>	<u>ORGANIZATION</u>	<u>NO. OF COPIES</u>	<u>ORGANIZATION</u>
2	MCDONNELL-DOUGLAS HELICOPTER CO ATTN D VAN OSTEEN R WATERFIELD MAIL STATION D216 500 E MCDOWELL RD MESA AZ 85205	1	ATLANTIC RESEARCH CORP ATTN MARK FRIEDLANDER 5945 WELLINGTON ROAD MS G787 GAINESVILLE VA 22065
1	FN MANUFACTURING INC ATTN GEORGE KONTIS POST OFFICE BOX 24257 COLUMBIA SC 29224	2	UNIVERSITY OF VIRGINIA DEPT OF MECH AND AEROSPACE ENGINEERING ATTN H G WOOD III J MORTON CHARLOTTESVILLE VA 22901
2	ARROW TECH ASSOCIATES INC ATTN ROBERT WHYTE WAYNE HATHAWAY 1233 SHELBURNE ROAD SUITE D8 SOUTH BURLINGTON VT 05403		<u>ABERDEEN PROVING GROUND</u>
1	GEORGIA INST OF TECHNOLOGY THE GEORGE W WOODRUFF SCHOOL OF MECHANICAL ENGINEERING ATTN DR G P NEITZEL ATLANTA GA 30332	2	DIRECTOR US ARMY RESEARCH LABORATORY ATTN AMSRL CI LP (TECH LIB) BLDG 305 APG AA
1	UNITED DEFENSE LP ATTN SUZANNE DAVISON ARMAMENT SYSTEMS DIVISION 4800 EAST RIVER RD (MAIL STOP M239) MINNEAPOLIS MN 55421	2	DIR USAMSAA ATTN AMXSY D W BROOKS R CONROY
1	OLD DOMINION UNIVERSITY MATHEMATICS DEPARTMENT ATTN DR CHARLIE COOKE NORFOLK VA 23508	5	CDR USAATC ATTN STECS AAL M MAULE STECS AS LA S WALTON STECS DA P PAULES STECS AS HP J ANDREWS BLDG 400
1	SCITEC INC ATTN ALEX ZISLAN 100 WALL STREET PRINCETON NJ 08540	2	CDR USATECOM ATTN AMSTE TE R MR KEELE AMSTE TA R W MARSHALL RYAN BLDG
1	LOS ALAMOS NATIONAL LAB ATTN THOMAS DAVIS GROUP WX 4 MS G787 LOS ALAMOS NM 87545	1	DIR AMC INT MAT EVAL DIV ATTN AMCICP IM R BLOOM
1	OLIN CORPORATION ATTN STEPHAN FAINTICH PO BOX 222 ST MARKS FL 32355	4	DIR USAARDEC ATTN SMCAR FSF T R LIESKE J MATTS R PUHALLA J WHITESIDE FIRING TABLES BRANCH BLDG 120
		40	DIR USARL ATTN AMSRL WM I MAY AMSRL WM P A HORST E SCHMIDT AMSRL WM PA T MINOR G KELLER M NUSCA AMSRL WM PC R FIFER

NO. OF
COPIES ORGANIZATION

AMSRL WM PD B BURNS
AMSRL WM W C MURPHY
AMSRL WM WB W D'AMICO
 B DAVIS
 F BRANDON
 G BROWN
AMSRL WM WC J BORNSTEIN
 R VON WAHLDE
AMSRL WT PB K FANSLER (5)
 P PLOSTINS
 D WEBB
 G COOPER (2)
 M BUNDY
 B PATTON
 K SOENCKSEN
 V OSKAY
 J GARNER
 P WEINACHT
 B GUIDOS
 H EDGE
 J SAHU
 A MIKHAIL
 A ZIELINSKI
AMSRL HR SD J KALB
AMSRL SC C C NIETUBICZ
AMSRL SC CC A CELMINS

REPORT DOCUMENTATION PAGE

Form Approved
OMB No. 0704-0188

Public reporting burden for this collection of information is estimated to average 1 hour per response, including the time for reviewing instructions, searching existing data sources, gathering and maintaining the data needed, and completing and reviewing the collection of information. Send comments regarding this burden estimate or any other aspect of this collection of information, including suggestions for reducing this burden, to Washington Headquarters Services, Directorate for Information Operations and Reports, 1215 Jefferson Davis Highway, Suite 1204, Arlington, VA 22202-4302, and to the Office of Management and Budget, Paperwork Reduction Project (0704-0188), Washington, DC 20503.

1. AGENCY USE ONLY (Leave blank)		2. REPORT DATE August 1997	3. REPORT TYPE AND DATES COVERED Final	
4. TITLE AND SUBTITLE Yaw Card Perturbation of Projectile Dynamics			5. FUNDING NUMBERS PR: 1L162618AH80	
6. AUTHOR(S) Cooper, G. R.; Fansler, K. S.				
7. PERFORMING ORGANIZATION NAME(S) AND ADDRESS(ES) U.S. Army Research Laboratory Weapons & Materials Research Directorate Aberdeen Proving Ground, MD 21010-5066			8. PERFORMING ORGANIZATION REPORT NUMBER	
9. SPONSORING/MONITORING AGENCY NAME(S) AND ADDRESS(ES) U.S. Army Research Laboratory Weapons & Materials Research Directorate Aberdeen Proving Ground, MD 21010-5066			10. SPONSORING/MONITORING AGENCY REPORT NUMBER ARL-TR-1431	
11. SUPPLEMENTARY NOTES				
12a. DISTRIBUTION/AVAILABILITY STATEMENT Approved for public release; distribution is unlimited.			12b. DISTRIBUTION CODE	
13. ABSTRACT (Maximum 200 words) Using an impulse or Dirac delta approach, the stability and growth of yaw for a spin-stabilized projectile as it transits a yaw card range is investigated. The card-induced changes in the complex yaw arm amplitudes and phases are expressed as difference equations. For a yaw card range with uniform spacings, the solutions to the general difference equations yield the magnitude and phase values for the complex yawing arms as a function of the card index number. A stepwise encounter with a yaw card reduces the epicyclical phase values across the yaw card. The parameters for the solution include encounter phase value at the entrance of the range, the characteristics of the yaw card, and the distance between the cards. Critical curves separating stable and unstable flight are presented as a function of yaw card spacing and a stability parameter that depends upon both the flight characteristics of the projectile and the card material and thickness. Quasi-universal curves of a transformed epicyclical phase encounter value versus a normalized epicyclical phase reduction value are graphically presented.				
14. SUBJECT TERMS flight mechanics particle trajectory yaw card flight stability projectile stability			15. NUMBER OF PAGES 44	
			16. PRICE CODE	
17. SECURITY CLASSIFICATION OF REPORT Unclassified	18. SECURITY CLASSIFICATION OF THIS PAGE Unclassified	19. SECURITY CLASSIFICATION OF ABSTRACT Unclassified	20. LIMITATION OF ABSTRACT	